Chicxulub as an Oblique Impact. Peter H. Schultz, Department of Geological Sciences, Brown University, Providence, RI 02912.

Introduction: The discovery (1), confirmation (2), timing (3), and analyses of the geophysical expression (2, 4) of the Chicxulub structure establish a major impact at the end of the Cretaceous. These data also provide important clues for the nature of the collision based on analogy with well-preserved craters on other planets and an understanding of the impact process. Previous studies speculated about the effects a major oblique impact on the Earth (1, 2) but the new geophysical data contain substantive evidence that Chicxulub was formed by an object 10-15 km in diameter at an angle of 20-30° from the southeast. Such a perspective is important for appreciating the devastating atmospheric/biospheric stress.

Oblique Impacts--Mapping Time into Space: The impact cratering process can be subdivided into three stages (5): penetration, excavation, and modification. These stages are witnessed in laboratory and computational experiments of vertical impacts, but are largely masked in the final crater appearance as each successive stage supersedes the next. Oblique impacts, however, spread these time-dependent stages along the trajectory and preserve related asymmetries. *Penetration:* The penetration stage for oblique impacts changes with time along the trajectory. Laboratory experiments using the NASA-Ames Vertical Gun Range (AVGR) reveal that projectile failure occurs prior to significant penetration of the surface. Spallation of the uppermost surface results in a string of fragments along the downrange trajectory for very low angle impacts (< 10°). Higher impact angles (15-30°) result in ricochet rays subtending larger angles with increasing impact angle (from horizontal). For example, the Rio Cuarto crater in Argentina and Messier exhibit ricochet rays subtending only 5-10°, consistent with very low impact angles. Schrödinger (Moon) exhibits a pronounced pair of chains subtending about 45°, consistent with a higher angle. The 2-ring basin Bach (Mercury, Fig. 2a) and multi-ring lunar basin Orientale (Fig. 2b) exhibit similar patterns. In each case, the chains converge close to the first point of contact. The rate of energy transfer to the target depends on impact angle and velocity. Hypervelocity collisions result in the greatest penetration uprange with shallower penetration downrange due to "sibling" (projectile ricochet) collisions at lower angles. This early penetration stage is recognized both in laboratory experiments and at much larger planetary scales by: secondary and sibling crater chains extending back uprange; greatest shock damage at depth (penetration) but least surface failure uprange; elongate or breached penetration zones (expressed as elongate or breached central rings at planetary scales); downrange impact melt and vapor condensate preserving a portion of the impactor momentum; and asymmetric profile (deepest uprange in simple craters; uprange-offset central peaks in complex craters). The dimensions of the penetration zone have been found to be independent of impact angle and can be used to estimate impactor size consistent with other scaling relations (6, 7). Due to gravity-limited growth, the penetration stage comprises an increasing fraction of the excavation stage (20%) at very large scales (> 100 km). *Excavation:* The energy transfer from impactor to target resembles a moving source for oblique impacts. The pronounced penetration asymmetry becomes more symmetrical during the later stage of ballistic excavation. Consequently, a more radial pattern of ejecta emplacement centered downrange superposes the earlier non-radial pattern reflecting impactor failure centered uprange. The center of symmetry, however, is offset downrange from the region of deepest penetration. Fracture patterns generated by oblique impacts at the AVGR dramatize these two centers of symmetry (Fig. 1). The outer failure zone forms an incomplete, subarcuate fracture uprange but is centered downrange from the region of maximum penetration. Depth of excavation decreases with impact angle and may be significantly less downrange. *Modification:* The modification stage is difficult to document directly at laboratory scales. Nevertheless, this stage should reflect responses to both the region of deepest penetration and near-surface failure (Fig. 1). Deeper penetration results not only in rebound offset uprange but also enhanced rim/wall collapse uprange for craters above a critical size (6). This "circularizes" the crater outline in part, but the shallow depths of excavation downrange undergo less readjustment.

Chicxulub: The geophysical patterns and surface expressions of Chicxulub (2, 4) are consistent with formation by an oblique impact from the southeast. The inner gravity high is relatively symmetrical but is flanked by a horse shoe-shaped low with extensions northeast and northwest. Such a pattern is consistent with asymmetric excavation preserving the early stages of penetration and failure by an impactor from the southeast at an angle from 20-30°. Similar patterns are found on Venus (6), Mercury, and the Moon (see Fig. 2). The limits of the central gravity high provide a signature of the penetration zone, which may provide a measure of the impactor. The only analog clearly linking a gravity high to preserved crater features in the 2-ring basin Grimaldi on the Moon (8). The dimensions of this central anomaly closely match the diameter of the interior peak ring, which falls on the empirical relation between diameters of other central relief structures (Fig. 3a). Plotting the diameter of gravity highs of other terrestrial craters onto the diameter of central peaks and rings of craters on Venus (Fig. 3b) reveals a consistent relation. On this plot, the 60 km diameter of the central gravity high of Chicxulub suggests that its crater diameter should be about 130-150 km. Although this is considerably smaller than the outermost rings of Chicxulub (4), the disparity is proposed to reflect more extensive rim/wall collapse and failure zones uprange that can extend well beyond the original excavation rim, as on the Moon and Mars. Scaling of the penetration zones and central peak

© Lunar and Planetary Institute • Provided by the NASA Astrophysics Data System

Chicxulub as an Oblique Impact, P.H. Schultz

dimensions (6, 7) yield an impactor size between 10 and 15 km in diameter depending on the assumed impact velocity. If these interpretations are correct, then the northern hemisphere could have been subjected to much greater atmospheric stress. Moreover, this region would have received multi-staged impact products reflecting separate stages of impactor-driven vaporization, high-speed ballistic ejecta and secondary products, and dispersed target vapor/melt products.

(1) Penfield, G.T. and Camargo, Z.A. (1981), *Mtg. Soc. Explor. Geophys. Abstr., 51*, 37. (2) Hildebrand, A.R. *et al.* (1991), *Geology, 19*, 867-871. (3) Sharpton, V.L. *et al.* (1992), *Nature, 359*, 819. (4) Sharpton, V.L. *et al.* (1993) *Science, 261*, 1564-1567. (5) Gault, D.E. et al. (1968) in *Shock Metamorphism of Natural Materials*, pp. 87-100, Mono Books, Baltimore, MD. (6) Schultz, P.H. (1992), *J. Geophys. Res., 97*, 16,183-16,248. (7) Schultz, P.H. and Gault, D.E. (1993), *Lunar Planet. Sci. XXIV*, 1257-1258. (8) Phillips, R.J. and Dvorak, J.(1981), in *Multi-Ring Basins*, pp. 91-104, Pergamon, NY. (9) Scott, D.H., McCauley, J.F., and West, M.N. (1977), US Geol. Survey Map I-1034.

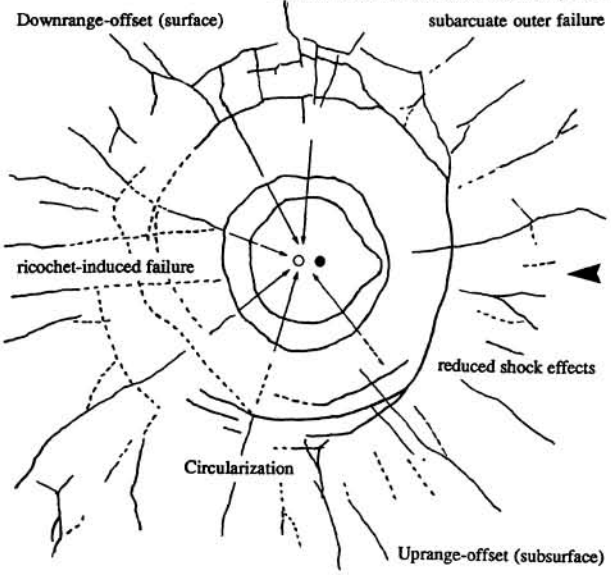

Figure 1. Fracture pattern created in a dry-ice block from a 30° impact (from horizontal) by a 0.635 cm aluminum sphere at 1.6 km/s. The deepest penetration (solid dot) occurs uprange but the radial and concentric failure pattern at the surface is centered downrange. An outer subarcuate fracture reflects the combined effects of reduced shock uprange and the time-dependent energy coupling downrange, thereby producing a mach-like boundary cone in the target (but pointing uprange). Similar patterns occur in basalt and lucite targets.

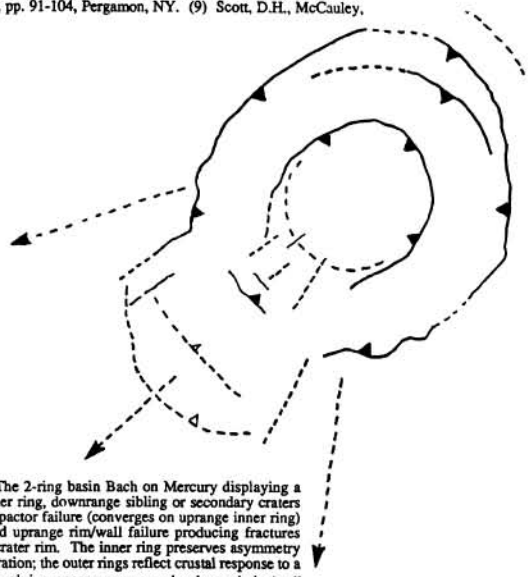

Figure 2a. The 2-ring basin Bach on Mercury displaying a breached inner ring, downrange sibling or secondary craters related to impactor failure (converges on uprange inner ring) and enhanced uprange rim/wall failure producing fractures beyond the crater rim. The inner ring preserves asymmetry during penetration; the outer rings reflect crustal response to a time/space-evolving energy source and enhanced rim/wall collapse uprange.

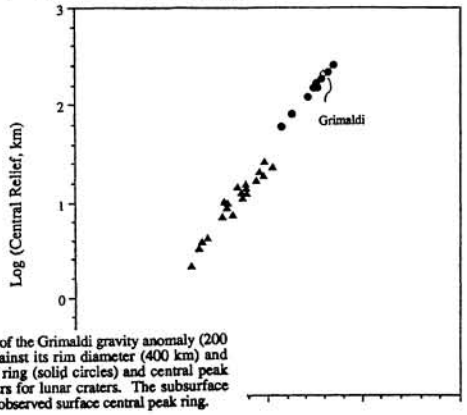

Figure 3a. The diameter of the Grimaldi gravity anomaly (200 km) from (8) plotted against its rim diameter (400 km) and superposed on the inner ring (solid circles) and central peak (solid triangles) diameters for lunar craters. The subsurface uplift correlates with the observed surface central peak ring.

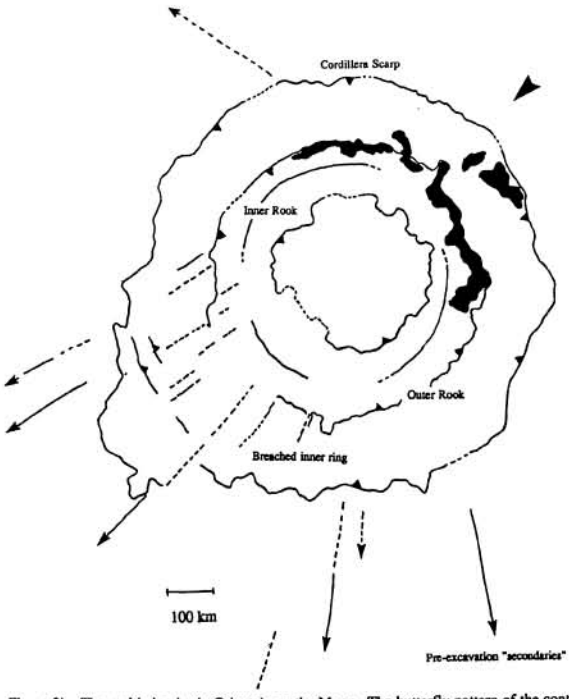

Figure 2b. The multi-ring basin Orientale on the Moon. The butterfly pattern of the continuous ejecta deposits of Orientale suggest an oblique impact (9). This is further indicated by early-stage "secondaries" converging on the uprange inner Rook, the downrange breach of the Rook ring, downrange extension of the Cordillera, and deep-seated failure uprange leading to mare emplacement (consistent with enhanced uprange collapse).

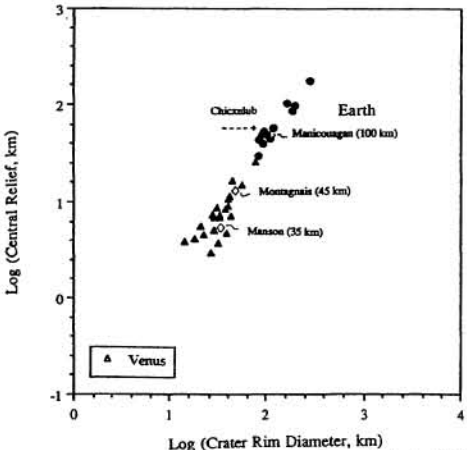

Figure 3b. Central gravity anomaly diameters for three terrestrial craters (open triangles) plotted with central peak (solid triangles) and peak ring (solid circles) diameters on Venus against their rim diameters. The diameter of the central gravity anomaly of Chicxulub is consistent with an uplift diameter only slightly larger than Manicouagan. The additional larger diameter rings at Chicxulub may reflect failure beyond the excavation crater rim, rather than the limit of the excavation crater.

© Lunar and Planetary Institute • Provided by the NASA Astrophysics Data System